

## Realization of a Particle-in-a-Box: Electron in an Atomic Pd Chain

N. Nilius,<sup>†</sup> T. M. Wallis,<sup>‡</sup> and W. Ho\*

*Department of Physics and Astronomy and Department of Chemistry, University of California, Irvine, California 92697-4575*

*Received: June 27, 2005; In Final Form: July 28, 2005*

Well-defined Pd chains were assembled from single atoms on a NiAl(110) surface with the tip of a scanning tunneling microscope. The electronic properties of the chains were determined by spatially resolved conductance measurements, revealing a series of quantum well states with parabolic dispersion. The particle-in-a-box states in Pd chains show higher onset energy and larger effective mass than those in Au chains investigated before, reflecting the influence of elemental composition on one-dimensional electronic systems. The intrinsic widths and spectral intensities of Pd induced states provide information on lifetime and spatial localization of states in the atomic chain.

One-dimensional (1D) chains of single atoms represent a model system for investigating the relationship between structural and electronic properties of matter.<sup>1–4</sup> The geometry of atomic chains is well-described by the lattice constant between neighboring atoms. If electronic properties of the isolated atom can be reduced to a single orbital with given energy and spatial extension, the electronic structure of the chain results from the overlap of these orbitals, leading to the formation of quantum well states. The hybridization efficiency between neighboring orbitals determines dispersion and intrinsic width of the electronic levels in the chain. For chains deposited on a support, an additional influence of the substrate electronic structure has to be considered.<sup>5</sup>

The fascinating simplicity of such model systems is accompanied by considerable difficulties in their experimental realization. Nonlocal preparation techniques, such as self-assembly of linear structures, decoration of step edges, or adsorption on template surfaces, do not allow fabrication of chains with atomic precision.<sup>6–8</sup> Neither the exact number of atoms nor their position and chemical identity can be controlled in these aggregates. In recent experiments, the assembly of atomic chains has been demonstrated with a scanning tunneling microscope (STM).<sup>9–12</sup> The technique utilizes attractive forces between the tip apex and a single adatom at small tip–sample distances to induce controlled motion and positioning of the adatom on the surface. Atom manipulation with the STM has been employed to assemble well-defined chains from single Au atoms on NiAl(110). The chain formation initiates the development of quantum well states, which originate from the overlap between neighboring Au 6sp orbitals.<sup>13,14</sup> The states show a parabolic dispersion as a function of wavenumber, demonstrating the 1D character of the electronic system.

The experiments described in this paper focus on the influence of chemical composition on the electronic structure of atomic chains. For that purpose, Au atoms have been substituted by Pd atoms in the chain-building process. The two elements show distinct differences in their single-atom properties. The Au 6sp orbital, responsible for the formation of quantum well states in Au chains, is occupied by a single electron, whereas the Pd 5sp is empty and the highest occupied orbital has d character. Further deviations in the electronic structure can be expected from the different spatial extension of Au and Pd orbitals. As the geometric structure of Au and Pd chains is fixed by the lattice constant of the NiAl(110) support, changes in the electronic behavior directly reflect the influence of elemental composition of the monoatomic chains.

The experiments were performed in an ultrahigh-vacuum STM operated at 12 K.<sup>15</sup> The NiAl(110) surface was prepared by cycles of Ne<sup>+</sup> sputtering and annealing to 1300 K. The surface contains alternating Al rows and Ni troughs with an interatomic spacing of 2.89 Å along the rows. Pd atoms were evaporated from an alumina crucible and deposited at 12 K onto the surface. The single atoms were imaged as round protrusions, adsorbed on Ni–Ni or Al–Al bridge sites. The strong preference of Au and Ag atoms for the Ni–Ni position was not observed for Pd.<sup>13</sup> Adatoms could be moved across the surface by operating the STM at small gap resistance ( $V/I$ ), equivalent to a small tip–adatom separation. Manipulation of single Pd atoms became possible below 50 kΩ gap resistance. The onset resistance for Au manipulation was 3 times larger, indicating stronger Pd interaction with the NiAl surface. Chains containing up to 20 Pd atoms were constructed along the Ni troughs of the NiAl surface (Figure 1). The interatomic distance in the chain amounts to 2.89 Å corresponding to the distance between Ni–Ni bridge sites. In comparison, the nearest-neighbor distance in bulk Pd is 2.75 Å. Because of the strong overlap of atomic wave functions, individual Pd atoms in the chains were not resolved, and chains appeared with uniform height in STM topographic images.

\* To whom correspondence should be addressed. E-mail: wilsonho@uci.edu.

<sup>†</sup> Present address: Fritz-Haber-Institut der MPG, Faradayweg 4-6, 14195 Berlin.

<sup>‡</sup> Present address: National Institute of Standards and Technology, Boulder, CO 80305.

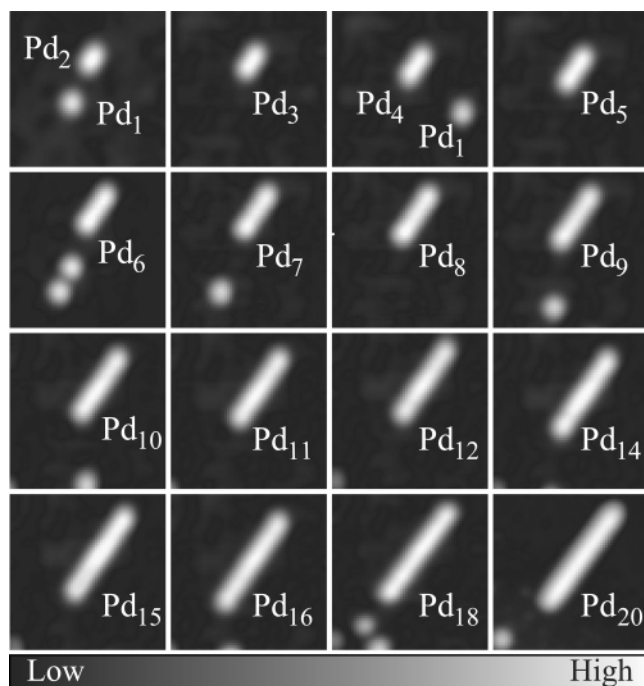


**Figure 1.** Assembly of individual Pd atoms to fabricate a Pd<sub>20</sub> chain on NiAl(110), using atom manipulation techniques with the tunneling gap set at  $V_{\text{sample}} = 2$  mV and  $I = 45$  nA. The images were taken at  $V_{\text{sample}} = 2.0$  V,  $I = 1.0$  nA. Each image is  $75 \text{ \AA} \times 75 \text{ \AA}$ .

A measure of the local density of states (LDOS) in atomic chains was obtained by detecting the differential conductance ( $dI/dV$ ) with lock-in technique and open feedback loop. The  $dI/dV$  spectra of single Pd atoms on Ni–Ni bridge sites show a distinct peak at 2.8 V, which is absent in spectra taken above the bare NiAl surface (Figure 2).<sup>16</sup> The formation of a Pd dimer along the Ni rows leads to a splitting of the resonance into two peaks at 2.05 and 2.55 V. The addition of more atoms to the chain induces a continuous red-shift of the low-energy  $dI/dV$  peak. The corresponding peak position is 1.91 V for Pd<sub>3</sub>, 1.75 V for Pd<sub>4</sub>, and 1.66 V for Pd<sub>5</sub>, and converges to 1.51 V in a 20-atom Pd chain (Figure 2). The peak energy exhibits an  $L^{-2}$  dependence as a function of chain length  $L$ . The electronic structure of Pd chains shows a similar length evolution as observed for Au chains.<sup>9</sup> However, absolute peak energies are distinctively different. The  $dI/dV$  resonance for a single Au atom is detected at 1.95 V, which corresponds to a red-shift of 0.85 V with respect to the Pd monomer. Similar shifts affect the  $dI/dV$  peaks in the atomic chains, where the lowest-energy resonance downshifts from 1.51 V in Pd<sub>20</sub> to 0.75 V in Au<sub>20</sub>. Furthermore, a minimum line width of 0.10 V is determined for  $dI/dV$  peaks in Pd chains, while Au induced states have an intrinsic width of more than 0.25 V.

Figure 3 shows a series of 21  $dI/dV$  spectra taken along the axis of a Pd<sub>20</sub> chain on NiAl(110), illustrating the spatial variation in differential conductance. The pronounced peak at 1.51 V dominates the spectra in the chain center. Resonances at higher energies exhibit distinct intensity oscillations along the chain, such as for the peak at 1.75 V. Cross-sections at a constant bias through the spectral series emphasize the modulations in conductance (Figure 4, center panel). The cuts reveal an increasing number of oscillations in the  $dI/dV$  signal with increasing sample bias. The  $dI/dV$  pattern can be visualized in  $dI/dV$  microscopic images, which map the differential conductance at fixed sample bias across the chain (Figure 4, outer panels).<sup>10</sup> The number of maxima and minima in the  $dI/dV$  signal perfectly agrees for spectroscopic and microscopic measure-

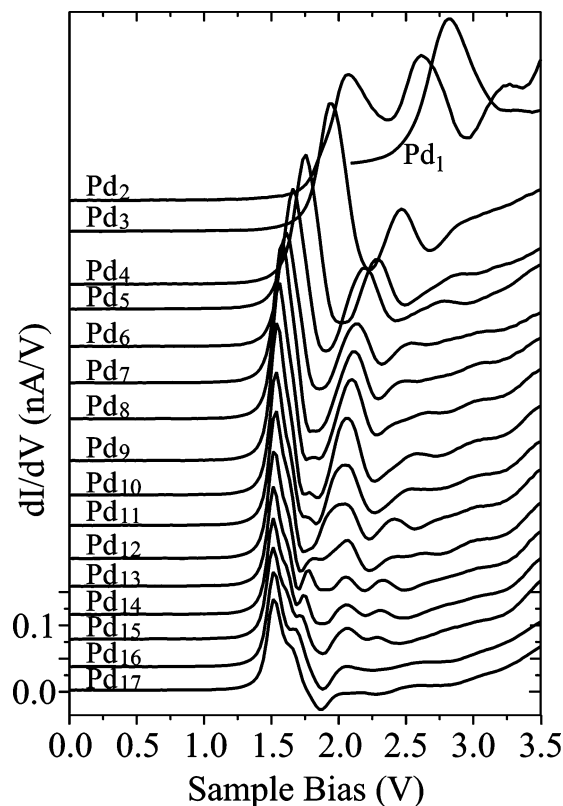


**Figure 2.**  $dI/dV$  spectroscopy of a single Pd atom and Pd chains containing between 2 and 17 atoms on NiAl(110). The gap was set with  $V_{\text{sample}} = 3.0$  V,  $I = 1.0$  nA. All spectra were taken in the chain center and are offset for clarity.

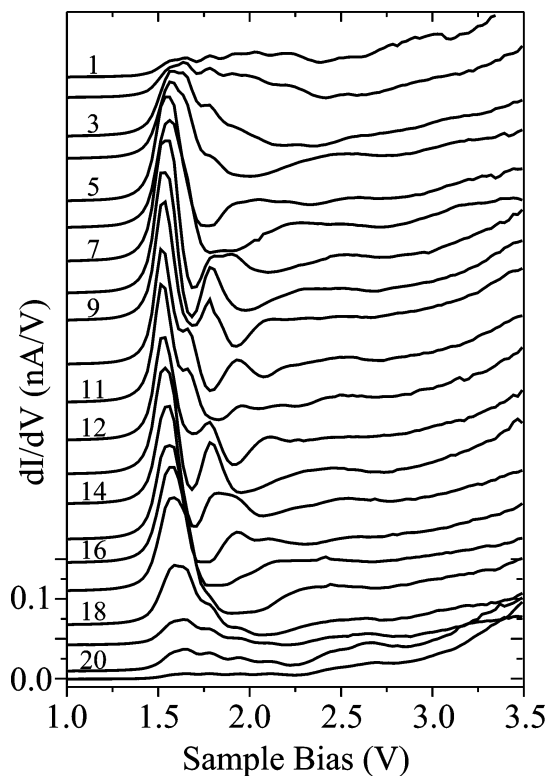


**Figure 3.** Series of  $dI/dV$  spectra taken at 21 equally spaced points along a Pd<sub>20</sub> chain on NiAl(110). The gap was set with  $V_{\text{sample}} = 3.0$  V,  $I = 1.0$  nA. Spectra are offset for clarity.

ments. The  $dI/dV$  image at 1.45 V shows a single maximum in the center of the Pd<sub>20</sub> chain. The number of oscillations increases

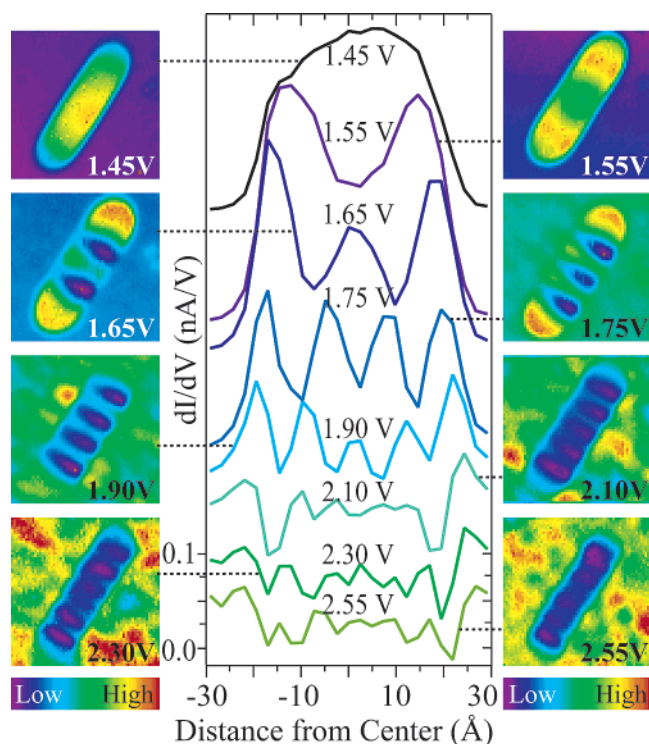


**Figure 4.** Cuts through the  $dI/dV$  spectra shown in Figure 3 and conductance images of a Pd<sub>20</sub> chain on NiAl(110), taken at  $I = 1.0$  nA and the indicated sample bias. Each image is  $65 \text{ \AA} \times 65 \text{ \AA}$ . Both techniques reveal a similar number of  $dI/dV$  oscillations along the chain axis, which increases with increasing sample bias.

to 2 at 1.55 V, 3 at 1.65 V and 4 at 1.75 V. Finally, 6 minima can be resolved at 2.30 V along the chain.

The  $dI/dV$  oscillations observed along the axis of the Pd<sub>20</sub> chain can be interpreted as standing wave patterns of quantum well states. The intensity patterns result from amplitude modulations of squared wave functions in the well and are most pronounced when the bias voltage matches the energy of an eigenstate in the chain. The energy positions of quantum well states are determined by fitting the experimental  $dI/dV$  oscillations as a function of sample bias to a 1D “particle-in-a-box” model. Wave functions in a 1D quantum well with infinite walls are sinusoids with wavenumber  $k_n = n\pi/L$ , depending on chain length  $L$  and quantum number  $n$ .<sup>17</sup> As experimental  $dI/dV$  patterns result from the overlap of neighboring quantum well states with finite width, a sum of squared sinusoids is used in the fitting procedure. A bias-dependent coefficient  $c_n$  accounts for the spectral weight of the different wave functions in the experimental spectra:<sup>17</sup>  $dI/dV(V) \propto \sum_n c_n(V) [\sin(k_n x)]^2$ . The maximum of  $c_n$  as a function of sample bias defines the energy of the corresponding quantum well state  $E_n$  (Figure 5A). For an ideal 1D quantum well, a parabolic dependence of the level energy on the wavenumber is expected:  $E_n(k) = E_0 + (\hbar^2/2m_{\text{eff}})k_n^2$ .<sup>17</sup> A plot of experimentally determined ( $E_n, k_n^2$ ) pairs reveals indeed a linear proportionality with a slope containing the effective electron mass  $m_{\text{eff}}$ . A fit to the data yields an effective mass of  $0.65m_e$  and onset energy  $E_0$  of 1.50 eV for states in a Pd<sub>20</sub> chain (Figure 5B,C).

Quantum well states in chains assembled from Au atoms on the NiAl surface are characterized by a smaller effective mass of  $0.5m_e$  and an onset energy shifted to 0.68 V.<sup>9,10</sup> Deviations in the electronic structure of the two chains reflect differences in adatom–adatom as well as adatom–support interactions. Their respective contributions can be analyzed by comparing the behavior of single atoms and chains on the NiAl surface.

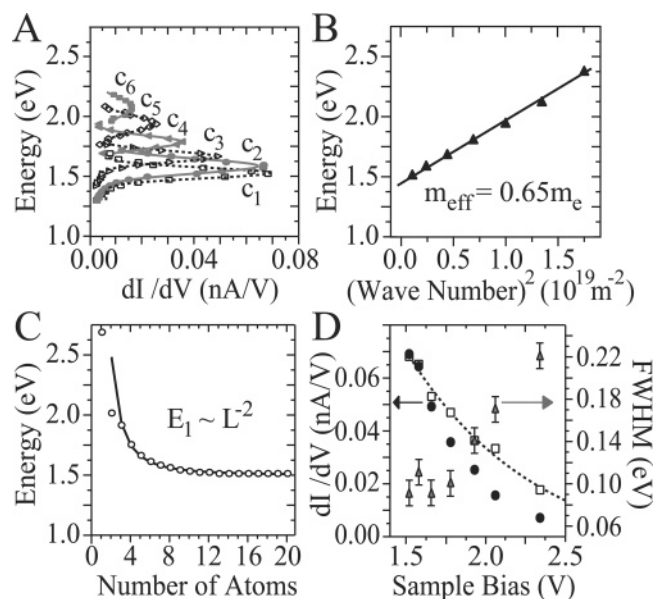


**Figure 5.** Coefficients  $c_n$  from fitting  $dI/dV$  oscillations in a Pd<sub>20</sub> chain to a 1D “particle-in-a-box” model. Each maximum in  $c_n$  defines the position of a quantum well state in the chain. (B) Energy position of quantum well states as a function of squared wavenumber for Pd<sub>20</sub> on NiAl(110). The slope of the linear fit to the data yields the effective electron mass of states in the quantum well. (C) Position of the lowest-energy  $dI/dV$  peak in Pd chains with increasing number of atoms (see Figure 2). Data points were fitted with an  $L^{-2}$  dependence on the chain length  $L$ . (D) Width ( $\blacktriangle$ ), maximum  $dI/dV$  intensity ( $\bullet$ ), and peak area in arbitrary units ( $\square$ ) of quantum well states in a Pd<sub>20</sub> chain, derived from the bias-dependent coefficients  $c_n$  shown in (A). The dashed line is an exponential fit, illustrating the decrease of the  $dI/dV$  peak area for states with higher quantum number  $n$ .

The 1.95 V resonance state observed for Au monomers was identified by density functional calculations as a hybridization of the Au 6sp orbital and NiAl electronic states.<sup>13</sup> The resonance represents the unoccupied part of a pair of bonding–antibonding states arising from the Au–NiAl interaction. The bonding state, calculated at  $-3.25$  V, is occupied by the initial Au 6s electron and an electron from the NiAl sp band. Because of its localization between Au adatom and NiAl surface, it could not be detected with STS. By assuming a similar binding mechanism for Pd atoms to NiAl(110), an additional electron has to be transferred into the bonding state, because the initial Pd 5sp orbital is empty. This missing electron could be donated from the Pd d states. Such reorganization of the electron configuration from  $\{\text{Pd } 4d^{10}, 5s^0\}$  to  $\{\text{Pd } 4d^9, 5s^1\}$  has previously been proposed for Pd adsorption on MgO and Pd–Au interaction in Pd<sub>1</sub>Au<sub>n</sub> cluster ions.<sup>18,19</sup> The energy cost for a  $d \rightarrow s$  promotion was determined to be approximately 0.8 eV for an isolated Pd atom, which would correspond to the observed shift in the resonance energy from Au<sub>1</sub> to Pd<sub>1</sub> monomers on NiAl(110).<sup>20,21</sup>

The coupling between neighboring electronic states induces a splitting of the single-atom resonance in ad-dimers on the NiAl surface. The interactions consist of direct orbital overlap and substrate-mediated coupling.<sup>13</sup> Both effects add to a total splitting of 0.8 eV in Au dimers assembled along the Ni rows. The corresponding Pd dimer shows a smaller splitting of 0.5 eV, which points to reduced interactions between the Pd induced states (Figure 2). An intuitive explanation attributes this reduction to a larger spatial confinement of the Pd 5sp orbital with respect to the Au 6sp state. The confinement leads to a smaller overlap between neighboring Pd orbitals and consequently decreases the level splitting in Pd dimers. The larger effective mass obtained for the quantum well states in Pd chains



is consistent with such a reduced hybridization between the Pd 5sp orbitals. Also, the observation of narrower  $dI/dV$  peaks in Pd chains compared to Au chains supports the assumption of weaker interactions between Pd induced electronic states. In bulk Pd, the larger confinement of Pd orbitals is compensated by a smaller lattice constant of 2.75 Å, whereas the value for bulk Au amounts to 2.89 Å.

An analysis of intrinsic widths and spectral intensities of  $dI/dV$  peaks in a Pd<sub>20</sub> chain provides information on lifetime and spatial extension of the quantum well states. Full-width-at-half-maximum (fwhm) and  $dI/dV$  intensity for each level  $E_n$  is deduced from the bias dependence of the coefficient  $c_n$  (Figure 5A). With increasing quantum number  $n$ , the  $dI/dV$  maximum decreases and states become broader (Figure 5D). The loss in peak height is not compensated by the increase in width, and also, peak areas attenuate with increasing bias. The continuous reduction in  $dI/dV$  intensity does not indicate a smaller LDOS of higher quantum well states, but reflects variations in the spatial extension of the corresponding wave functions perpendicular to the surface. The first wave function is dominated by one maximum in the chain center, which extends relatively far into the vacuum and allows effective tunneling from the tip apex. The second wave function has a node in the center, which leads to a smaller maximum amplitude in the two halves of the chain. The overlap with tip wave functions is reduced, and a weaker  $dI/dV$  signal is detected for the second quantum well state. With an increasing number of nodes, the wave functions become more confined perpendicular to the surface, and the associated electronic levels show reduced spectral intensity in STS. As a result, only the first 7 quantum well states could be identified for the Pd<sub>20</sub> chain on NiAl(110), although 20 states are expected from the interaction of the initial Pd orbitals.

Two major effects contribute to the observed broadening of Pd quantum well states with increasing sample bias (Figure 5D). In Fermi liquid theory, the lifetime of electronic excitations decreases as their energy separation from the Fermi level increases.<sup>22,23</sup> The reduction in lifetime and coherence length leads to the observed increase in fwhm of Pd resonance states with higher quantum number  $n$ . Additionally, the low-energy Pd<sub>20</sub> states lie in a pseudo gap of the NiAl bulk bands, extending from approximately 1.0 to 2.0 eV.<sup>24</sup> In this region of small LDOS, the interaction between the Pd orbitals and the NiAl bulk states is relatively weak. The coupling increases for Pd induced states above 2.0 V, causing an additional broadening of the  $dI/dV$  peaks.

The STM and STS experiments described in this paper provide a comprehensive picture of atomic Pd chains assembled on the NiAl(110) surface. Quantum well states in the chains

are characterized by an energy onset at 1.5 V and an effective electron mass of  $0.65m_e$ . Deviations from the electronic structure of Au chains on NiAl(110) are attributed to different electronic configuration and spatial extension of the initial Pd 5sp versus the Au 6sp orbital. The experiments demonstrate the influence of elemental composition on the electronic properties of structurally identical quantum systems.

**Acknowledgment.** The experiments were supported by the National Science Foundation, grant 0102887. N. Nilius gratefully acknowledges the Deutsche Forschungsgemeinschaft for a fellowship. We also thank M. Persson for many stimulating discussions.

## References and Notes

- (1) Lang, N. D. *Phys. Rev. B* **1995**, *52*, 5335.
- (2) Sanchez-Portal, D.; Artacho, E.; Junquera, J.; Ordejon, P.; Garcia, A.; Soler, J. M. *Phys. Rev. Lett.* **1999**, *83*, 3884.
- (3) de Maria, L.; Springborg, M. *Chem. Phys. Lett.* **2000**, *323*, 293.
- (4) Bahn, S. R.; Jacobsen, K. W. *Phys. Rev. Lett.* **2001**, *87*, 266101.
- (5) Yamada, T.; Yamamoto, Y. *J. Vac. Sci. Technol.* **1996**, *14*, 1243.
- (6) Persson, M. *Phys. Rev. B* **2004**, *70*, 205420.
- (7) Kuhnke, K.; Kern, K. J. *Phys.: Condens. Matter* **2003**, *15*, 3311.
- (8) Losio, R.; Altmann, K. N.; Himpfel, F. J. *Phys. Rev. Lett.* **2000**, *85*, 808.
- (9) Pampuch, B.; Rader, O.; Kachel, T.; Gudat, W.; Carbone, C.; Kläsger, R.; Bihlmayer, G.; Blügel, S.; Eberhardt, W. *Phys. Rev. Lett.* **2000**, *85*, 2561.
- (10) Nilius, N.; Wallis, T. M.; Ho, W. *Science* **2002**, *297*, 1853.
- (11) Wallis, T. M.; Nilius, N.; Ho, W. *Phys. Rev. Lett.* **2002**, *89*, 236802.
- (12) Nilius, N.; Wallis, T. M.; Ho, W. *Phys. Rev. Lett.* **2003**, *90*, 186102.
- (13) Fölsch, S.; Hyldgaard, P.; Koch, R.; Ploog, K. H. *Phys. Rev. Lett.* **2004**, *92*, 056703.
- (14) Nilius, N.; Wallis, T. M.; Persson, M.; Ho, W. *Phys. Rev. Lett.* **2003**, *90*, 196103.
- (15) Mills, G.; Wang, B.; Ho, W.; Metiu, H. J. *Chem. Phys.* **2004**, *120*, 7338.
- (16) Stipe, B. C.; Rezaei, M. A.; Ho, W. *Rev. Sci. Instrum.* **1999**, *70*, 137.
- (17) For Pd atoms on Al–Al bridge sites, a double resonance is detected with peaks at 2.4 and 3.1 V.
- (18) Kittel, C. *Introduction to Solid State Physics*; Wiley: New York, 1996.
- (19) Abbet, S.; Riedo, E.; Brune, H.; Heiz, U.; Ferrari, A.; Giordano, L.; Pacchioni, G. *J. Am. Chem. Soc.* **2001**, *123*, 6172.
- (20) Koyasu, K.; Mitsui, M.; Nakajima, A.; Kaya, K. *Chem. Phys. Lett.* **2002**, *358*, 224.
- (21) Valerio, G.; Toulhoat, H. *J. Phys. Chem.* **1996**, *100*, 10827.
- (22) Moore, C. E. *Table of Atomic Energy Levels*; US National Bureau of Standards: Washington, 1971.
- (23) The widths of Pd quantum well states show the energy dependence expected from the Fermi liquid theory:  $\text{fwhm} \propto (E_n - E_F)^2$ , demonstrating that the concept of Fermi liquids does not break down in this 1D system.
- (24) Echenique, P. M.; Pitarke, J. M.; Chulkov, E. V.; Rubio, A. *Chem. Phys.* **2000**, *251*, 1.
- (25) Lui, S. C.; Kang, M. H.; Mele, E. J.; Plummer, E. W.; Zehner, D. M. *Phys. Rev. B* **1989**, *39*, 13149.